Modelling Magnetic Confinement of Plasma in Toroidal Fusion Devices

Adam Knutsson

***Abstract*—In this report, a study of how the magnetic field provides confinement in a fusion device has been conducted. For this purpose, a model of the magnetic field at different positions inside the device has been developed. The magnetic field model is implemented using numerical software together with a simple description of the fusion plasma in order to calculate single charged particle orbits inside the device. The orbits are studied to examine how they are affected when the input parameters of the model is varied.**

The studies showed that there are two typical types of particle orbits: the trapped particle orbit and the passing particle orbit. The orbit type is related to the amount of parallel velocity with respect to the magnetic field: a large parallel velocity generates a passing particle orbit whilst a small parallel velocity generates a trapped particle orbit. The studies also investigates what happens to the confinement as the parallel velocity reach its limit between the trapped and passing particle orbit.

The studies also examines the relationship between the level of confinement and the plasma current. An increasing plasma current improves particle confinement and a simple model to describe this relationship is developed and tested.

This report is a bachelor thesis from the department of Fusion Plasma Physics, School of Electrical Engineering at KTH Royal Institute of Technology in Stockholm.

I. Introduction

THE global energy consumption is expected to double, alternatively fourfold, by the end of 2100 [1]. In order to supply the world with energy that is sustainable, considering both the environment and the economy, and to meet the increasing demand for power, there is an intense program being conducted in the field of energy research.

Fusion energy, which is the energy released due to the *mass defect* when light atomic nuclei are fused together to form heavier elements, may play a vital role in preventing the possible future energy crisis.

A wide variety of different fusion experiments is being conducted around the world where different materials and reactor types are being tested. The largest experiments, that will play an important role for the future of commercial fusion energy, is the International Thermonuclear Experimental Reactor (ITER) with a planned start of operations around 2020 and DEMO, a demonstration power plant with a planned start of operations around 2050 [2].

ITER will be constructed as a so called Tokamak, meaning that magnetic fields will be used to confine the plasma within a torus and thereby allowing the fusion reaction to take place without the extreme heat destroying the reactor vessel [3].

In this report, a model of the motion of a single charged particle confined within a magnetic field with symmetrical properties similar to those of a Tokamak, is developed, numerically implemented, and tested. The model is approximative with respect to the generation, and therefore also properties, of the magnetic field in such a device. The model is also approximative with respect to the physical construction of the reactor vessel, meaning that elements such as *limiters* and *divertors*, i.e. devices used for controlling the plasma exhaust and protecting the vessel walls [4], is not taken into account.

The developed model is used to perform a series of simulations that studies how the particle orbits depend on input parameters, such as the initial conditions of the particle and the driven plasma current.

II. Dynamics Modelling

A. Plasma Dynamics

Fusion reactions require extremely high temperature in order for the atomic nuclei of the fuel to overcome their natural repulsive force and fuse. The temperature required for efficient Deuterium-Tritium reaction is in the excess of 10^8 K [5]. The high temperature turns the Deuterium-Tritium fuel mixture into a so called plasma.

Plasma, sometimes referred to as the fourth state of matter, is a gas where the atoms inside are partially or fully ionized. A fully ionized plasma, which means that all the atoms in the plasma are ionized, has characteristics that have to be included when modeling the plasma itself.

Fusion plasmas are often fully ionized and have exceptionally high conductivity, typically many times that of an ordinary good conductor. This property can be explained with the fact that a plasma has a very low particle density, often orders of magnitudes smaller than that of a typical good conductor, and has free electrons with high mobility. The low density reduces the number of collisions between the particles, and this low collision rate makes the resistance of the plasma very small. The high conductivity also shields the plasma from static electric fields [5].

The low particle density and the low collision frequency makes the particles within the plasma exhibit so called *collision-less behavior*. This means that a plasma particle will not be significantly affected by other particles in the plasma during time scales shorter than the collision time described below [5].

If a fusion plasma is affected by a magnetic field, the particles will interact with the magnetic field as described by the Lorentz force. It is therefore sufficient to only study the motion of individual particles, e.g. a proton, and the surrounding magnetic field and to disregard its interaction with other particles in the plasma.

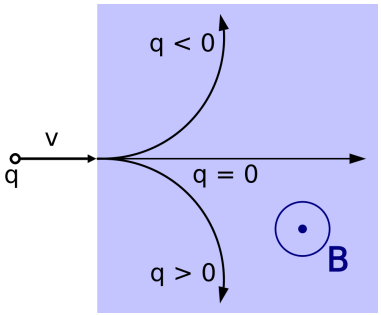

Fig. 1. A charged particle that enters a perpendicular, homogeneous magnetic field accelerates in perpendicular relationship to the magnetic field and velocity [6].

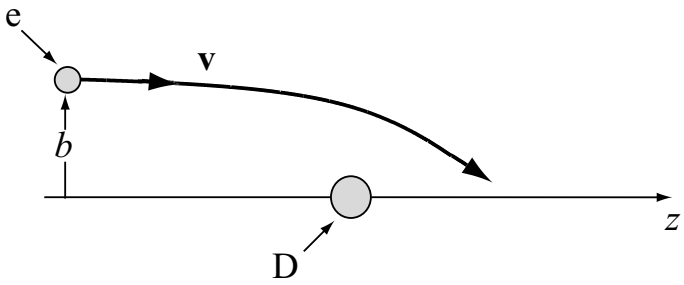

Fig. 2. An electron subjected to a Coulomb collision with a stationary Deuterium nucleus [5].

B. Particle Dynamics

A particle with charge q, moving with the speed $\vec{v}$, through a magnetic field, $\vec{B}$, and an electric field, $\vec{E}$, experience the Lorentz force described in (1).

$$\vec{F} = q\left(\left(\vec{v} \times \vec{B}\right) + \vec{E}\right) \tag{1}$$

Equation (1) states that the experienced force is the sum of two forces, one generated by the electric field, and the other generated by the motion within the magnetic field. Since fusion plasmas have very high conductivity, it is shielded from static electric field. And thus the electric field within the plasma is neglected. Particles will therefore only be affected by their motion relative to the magnetic field. If the remaining contribution from the Lorentz force is combined with Newton's second law of motion, which describes the relation between force, mass and acceleration, the differential equation (2) is generated.

$$\dot{\vec{v}} = \frac{q}{m}\left(\vec{v} \times \vec{B}\right) \tag{2}$$

Equation (2) states that the acceleration of a particle within the plasma is perpendicular to both the velocity and the magnetic field. This behaviour is illustrated in figure 1.

From figure 1 and equation (2) a very important fact is now realised: A particle moving perpendicular to a (locally) homogeneous magnetic field will start to gyrate around the field lines and form a circular path. This circular path has certain properties such as its radius, also called gyro radius or Larmor radius, and the number of revolutions the particle makes around the path in one second, also called the gyration frequency, f_g.

In order to motivate the earlier mentioned collision-less behaviour, the inverse of the gyration frequency, also called the gyration time, T_g, is studied for a proton

$$T_g = f_g^{-1} = \frac{2\pi m_p}{|q||\vec{B}|} \approx \frac{6.556}{|\vec{B}|} \cdot 10^{-8}. \tag{3}$$

For toroidal fusion devices such as Tokamaks the magnetic field is often in the order of Teslas, e.g. the TEXTOR Tokamak with a magnetic field strength of 3 T [7], which means that the gyration time for protons inside Tokamaks is of the order 10^{-8} s.

The gyration time is the smallest time scale that is taken into account in this report. If a particle is studied for only a small amount of gyrations, the particle's spatial position can be known with good accuracy. However, during longer time scales other effects need to be taken into account, such as Coulomb collisions and plasma turbulence. In this report, only the effect of Coulomb collisions are explained and discussed.

1) Coulomb Collisions: If the plasma is modelled as a gas of ions, each particle will generate an electric field according to Gauss's law. Two ions in proximity to each other will experience the Coulomb force that attracts or repel the ions to one another. The scalar expression for the magnitude of the Coulomb force is presented in (4).

$$|\vec{F}| = k_e \frac{|q_1 q_2|}{r^2} \tag{4}$$

Equation (4) states that the exerted force is large when the particles are close to one another, and is proportional to the inverse distance squared. Particles with different sign of the charge will attract and particles with equal sign of the charge will repel. The Coulomb force, combined with the fact that plasma has a low density and high temperature, makes the particle unlikely to preform classic kinetic collisions, i.e. collisions can be described by the particles physically bumping into one another like the balls in a game of pool. Instead, the particle will be subjected to a more slow type of collision, only noticeable after a series of cumulated Coulomb collisions. The low collision rate makes the particle change course on a time scale that is order of magnitude longer than that of the gyration time, and its effect is therefore neglected in this report.

C. Particle Guiding Centre

If a particle has started moving inside a magnetic field, its velocity may be divided into two components: perpendicular to the magnetic field, $v_\perp$, and parallel to the magnetic field, $v_\parallel$. The perpendicular component, as described earlier, forces the particle to gyrate and the parallel component makes the particle move along the field lines. The resulting particle motion will be a helical path following the magnetic field. If only the centre of this helical path is studied, it is referred to as the *guiding centre* path and it is usually parallel to the magnetic field lines. The guiding centre is the easiest way to understand how a particle moves with respect to the surrounding magnetic field. An example of a particle moving

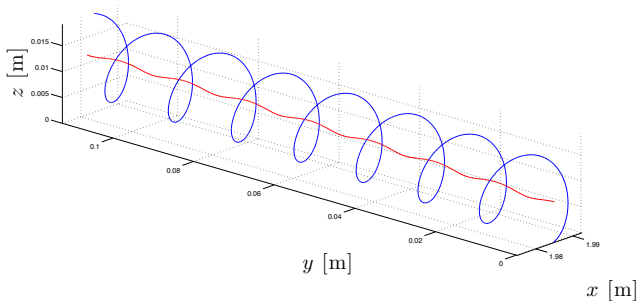

Fig. 3. Motion of a proton within an approximate Tokamak magnetic field. The helical path is the true path of the particle an the other path is the guiding centre.

through a magnetic field and its guiding centre is shown in figure 3.

D. Particle Initial Condition

In order to solve the differential equation described in section II-B it is essential that a particle is given an initial velocity for the motion to continue. A stationary charged particle within a time invariant magnetic field will remain stationary.

The high temperature of fusion plasmas results in a high thermal energy, often in the ranges of 10-40 keV for reaction between Deuterium and Tritium. When the energy, E, is known, and not large enough to generate relativistic motion, the magnitude of the particles velocity, $|\vec{v}|$, can be calculated using the definition provided by classical mechanics, described in equation (5).

$$E = \frac{1}{2}m|\vec{v}|^2 \quad \Leftrightarrow \quad |\vec{v}| = \sqrt{\frac{2E}{m}} \tag{5}$$

Since equation (5) only computes the magnitude of the velocity vector, further relationships between the particleäs motion relative to the magnetic field is required.

Since the toroidal magnetic field in a Tokamak is larger than the poloidal magnetic field, which will be shown in section IV, a good first approximation of the magnetic field is a strictly toroidal field that lies in the (x, y)-plane. It is now possible to define the pitch angle, φ_p, which is $\varphi_p = \pi/2 - \bar{\varphi_p}$ and $\bar{\varphi_p}$ is the angle between the velocity vector, $\vec{v}$, and the approximate magnetic field, $\vec{B}$ [1].

However, the relationship that describes the pitch angle in (6) is approximative and assumes that the magnetic field can be written on the form $\vec{B} = B\vec{e}_y$ and the particle initial position is at $y = 0$.

$$\begin{cases} v_x = \sqrt{\frac{2E}{m}}\cos\varphi_p \\ v_y = \sqrt{\frac{2E}{m}}\sin\varphi_p \end{cases} \tag{6}$$

III. Geometric Modelling

In order to compute the magnetic field inside a toroidal fusion device, e.g. a Tokamak, it is important to analyse the geometric properties of the torus, which can be used as an approximation of the reactor vessel in such devices.

[1] $\bar{\varphi_p}$ is the conventional definition of the pitch angle. In this report the angle $\varphi_p = \pi/2 - \bar{\varphi_p}$ is used instead.

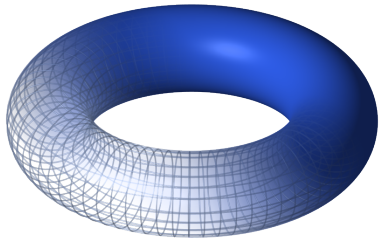

Fig. 4. A ring torus [8].

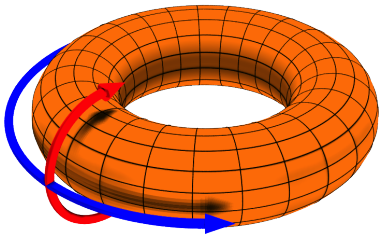

Fig. 5. Representation of toroidal angle (long arrow) and poloidal angle (short arrow) [9].

A torus is the shape generated when the centre of a circle with radius R_{mi} is rotated around another circle with radius R_{ma}. Here R_{ma} is refereed to the major radius and R_{mi} is referred to as the minor radius. An example of a torus is displayed in figure 4. If $R_{\text{ma}} > R_{\text{mi}}$ the torus is referred to as a ring torus, and this is the approximate shape of a toroidal fusion device.

A. Toroidal Coordinate System

The symmetrical properties of the torus makes it possible to define a coordinate system more suitable for describing points within the torus rather than using classic Cartesian coordinates. The toroidal coordinate system is based on two angles and a distance and is defined as follows:

- The toroidal angle, ϕ, is defined as the angle that increases or decreases as an object moves through the torus. It lies in the interval $0 \leq \varphi < 2\pi$ and is represented by the long arrow in 5.
- The poloidal angle, θ, is defined as the angle that increases or decreases as an object moves along the inner wall of the torus. It lies within the interval $0 \leq \theta < 2\pi$ and is represented by the short arrow in figure 5.
- The radius, r, is defined as the distance from the point to the central axis, i.e. the centre on the circular toroidal cross section in this report.

The relationship between the toroidal coordinate system and the classic, Cartesian coordinate system is described by equation system (7)

$$\begin{cases} x(\phi,\theta,r) = (R_{\text{ma}} + r\cos\theta)\cos\phi \\ y(\phi,\theta,r) = (R_{\text{ma}} + r\cos\theta)\sin\phi \\ z(\phi,\theta,r) = r\sin\theta \end{cases} \tag{7}$$

where R_{ma} is the major radius of the torus and treated as a constant.

B. Toroidal Unit Vectors

With the toroidal coordinate system defined, it is important to find the basis vectors of the toroidal coordinate system expressed as linear combinations of the standard basis. This is essential, since the differential equation (2) uses the cross product defined in the standard basis, while the magnetic field, which will be shown in section IV, is much easier to describe in the toroidal basis.

Since the toroidal coordinate system can be regarded as a curvilinear coordinate system relative to the standard basis, the new basis vectors can be computed according to equation (8) [10].

$$\vec{e}_\phi = \frac{\partial x(\phi,\theta,r)}{\partial \phi}\,\hat{e}_x + \frac{\partial y(\phi,\theta,r)}{\partial \phi}\,\hat{e}_y + \frac{\partial z(\phi,\theta,r)}{\partial \phi}\,\hat{e}_z \tag{8}$$

The vector $\vec{e}_\phi$ is the vector that has the same direction as the unit vector $\hat{e}_\phi$. However, it is scaled and is possibly not a unit vector since its length may be $|\vec{e}_\phi| \neq 1$ and requires normalization.

In equation (8) the computation of the new basis vector direction $\vec{e}_\phi$ is described. The process is the same for computation of $\vec{e}_\theta$ and $\vec{e}_r$, though the derivatives are exchanged to $\frac{\partial}{\partial\theta}$ and $\frac{\partial}{\partial r}$, respectively. Performing the computation generates the directions of the basis vectors accordingly

$$\vec{e}_\phi = \begin{pmatrix}\vec{e}_x & \vec{e}_y & \vec{e}_z\end{pmatrix} \cdot \begin{pmatrix} -r\sin\phi\cos\theta - R_{\text{ma}}\sin\phi \\ r\cos\phi\cos\theta + R_{\text{ma}}\cos\phi \\ 0 \end{pmatrix} \tag{9}$$

$$\vec{e}_\theta = \begin{pmatrix}\vec{e}_x & \vec{e}_y & \vec{e}_z\end{pmatrix} \cdot \begin{pmatrix} -r\cos\phi\sin\theta \\ -r\sin\phi\sin\theta \\ r\cos\theta \end{pmatrix} \tag{10}$$

$$\vec{e}_r = \begin{pmatrix}\vec{e}_x & \vec{e}_y & \vec{e}_z\end{pmatrix} \cdot \begin{pmatrix} \cos\phi\cos\theta \\ \sin\phi\cos\theta \\ \sin\theta \end{pmatrix}. \tag{11}$$

By normalizing the vectors $\vec{e}_\phi$, $\vec{e}_\theta$ and $\vec{e}_r$ the corresponding unit vectors $\hat{e}_\phi$, $\hat{e}_\theta$ and $\hat{e}_r$ are obtained.

C. Transformation of Coordinates

Equations (9) - (11) state, that in order to compute the new basis vectors, it is essential that the toroidal angle ϕ, the poloidal angle θ, and the radius r, are known. Since the particle position will be known in Cartesian coordinates, it is important to find a transformation from Cartesian coordinates to toroidal coordinates. This is solved by studying the equation system (7).

Through substitution, the toroidal angle can be obtained using (12).

$$\frac{y}{x} = \frac{\sin\phi}{\cos\phi} = \tan\phi \quad \Leftrightarrow \quad \phi = \arctan\frac{y}{x} \tag{12}$$

However, since the result domain of for the inverse tangent function in (12) only spans the interval $(-\frac{\pi}{2}, \frac{\pi}{2})$ while the toroidal angle is defined in the domain $(0, 2\pi]$, a numerical scheme is implemented for four-quadrant inverse tangent [11].

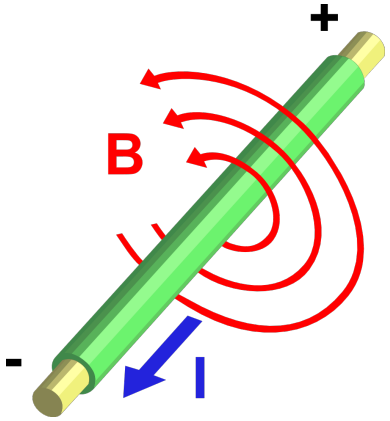

Fig. 6. A magnetic field generated from an electric current described by Ampere's law [12].

If the torus is located symmetrically around the z-axis with toroidal symmetry line in the $z = 0$ plane, the toroidal radius, r, can be obtained using Pythagoras theorem described in (13).

$$r = \sqrt{\left(R_{\text{ma}} - \sqrt{x^2+y^2}\right)^2 + z^2} \tag{13}$$

Finally, the poloidal angle can be obtained using equation (14).

$$z = r\sin\theta \quad \Leftrightarrow \quad \theta = \arcsin\frac{z}{r} \tag{14}$$

However, since the result domain of the inverse sine function only spans the interval $[-\frac{\pi}{2}, \frac{\pi}{2}]$, it is appropriate to rewrite it as a inverse tangent function, described in equation (15), and then implement the numerical scheme for four-quadrant inverse tangent again.

$$\theta = \arctan\left(\frac{z}{\sqrt{x^2+y^2} - R_{\text{ma}}}\right) \tag{15}$$

IV. Magnetic Modelling

In order to confine a fusion plasma within a Tokamak, a helical magnetic field that rotates along the torus is required. This is achieved by using a set of toroidal field coils and by driving a plasma current [5].

A. Toroidal Magnetic Field

The toroidal magnetic field is generated by using a series of coils symmetrically placed around the torus. The total current that flows around the torus in the poloidal direction is the current in each coil, I_C, multiplied by the number of windings per coil, N_W, and lastly multiplied by the number of coils, N. Using Ampere's law, the toroidal magnetic field inside the torus can be approximated using (16).

$$\oint_C \vec{B}\,d\vec{l} = \mu_0 \iint_S \vec{J}\,d\vec{S} = \mu_0 I_{\text{enc}} = \mu_0 N N_W I_C \tag{16}$$

Since the magnetic field is constant in the toroidal direction due to the nature of Ampere's law as shown in figure 6 the resulting toroidal magnetic field can be written on the form

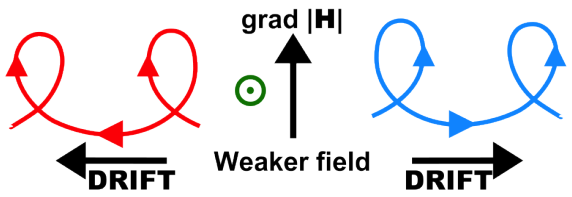

Fig. 7. The relationships between the drift motion, the magnetic field and the magnetic field gradient. The right drift motion is for a negatively charged particle and the left a positively charged particle [13].

$\vec{B} = B_t \hat{e}_\phi$ where B_t is calculated according to (17) using the relationship described in (16).

$$B_t(R) = \frac{\mu_0 N N_W I_C}{2\pi R} = B_t(x,y) = \frac{\mu_0 N N_W I_C}{2\pi\sqrt{x^2+y^2}} \tag{17}$$

B. Poloidal Magnetic Field

In order to generate a helical magnetic field, a poloidal field component perpendicular to the toroidal field is required. The poloidal magnetic field is generated by driving a plasma current, I_P, through the torus. The plasma current is driven using a solenoid placed at the centre of the torus, acting as the primary winding of a transformer, while the secondary winding is the plasma itself. If the resulting current flow is regarded as homogeneous inside the torus, the resulting current density within the torus is described by (18).

$$\vec{J} = \frac{I_P}{\pi R_{\text{mi}}^2}\,\vec{e}_\phi \tag{18}$$

Now, using Ampere's law, earlier described in (16), the poloidal magnetic field component at a distance r from the centre of the toroidal cross section can be approximately calculated using (19), by assuming the torus is bent only slightly.

$$B_p(r) = \frac{\mu_0 \pi r^2 |\vec{J}|}{2\pi r} = \frac{1}{2}\mu_0 r |\vec{J}| \tag{19}$$

The total, resulting magnetic field is now described as a sum of the toroidal and the poloidal field component in (20).

$$\vec{B} = B_t\vec{e}_\phi + B_p\vec{e}_\theta \tag{20}$$

C. Magnetic Drift

Because the resulting magnetic field, $\vec{B}$, is inhomogeneous, the particles within the plasma will experience a drift motion caused by the magnetic field gradient. The magnetic field is also curved, resulting in a curvature drift that is caused by the centrifugal force. The drift velocity of the particle caused by these two phenomena is described by equation (21) [5].

$$\vec{v}_D = \frac{v_\perp^2 + 2v_\parallel^2}{4\pi f_g}\frac{\vec{B}\times\nabla|\vec{B}|}{|\vec{B}|^2} \tag{21}$$

From equation (21) it is realised that the direction of the magnetic drift is perpendicular to both the magnetic field gradient and the magnetic field. This behaviour is described in figure 7.

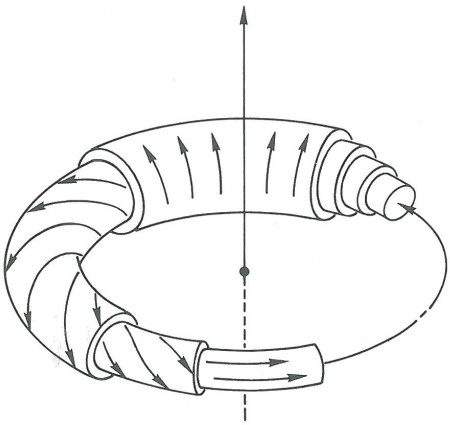

Fig. 8. Representation of different magnetic flux surfaces and the magnetic field associated with each surface in an RFP device [14].

D. Magnetic Flux surfaces

A magnetic flux surface is the surface generated when following a single magnetic field line inside a Tokamak for a large set of toridal revolutions. Since the helical magnetic field is bent around the torus, the poloidal component varies depending on poloidal angle, θ, and the field line will in general not end where the field line start after a fully performed toroidal revolution. Instead it starts to weave a so called *magnetic flux surface*.

The number of magnetic flux surfaces is infinite, and all surfaces will have a slightly different magnetic field associated with each surface. If the radius $r \to R_{\text{mi}}$, the poloidal field component will reach its maximum, and the resulting magnetic field helix will have a relatively small level of inclination. If the distance $r \to 0$ the poloidal field component will decrease, and the resulting magnetic field helix will have an increasingly high level of inclination and finally be infinite, i.e. the magnetic field will be strictly toroidal. The helical behaviour on different flux surfaces is depicted in figure 8.

E. The Safety Factor

In order to use a convenient expression for the relationship between the poloidal field strength and the toroidal field strength, the *safety factor* is used. It is defined as the number of toroidal revolutions the magnetic field requires in order to perform one poloidal revolution. A strong toroidal field results in a high safety factor and vice versa. The safety factor can be approximately defined according to equation (22) [5].

$$Q = \frac{rB_\phi}{R_{\text{ma}}B_\theta} \tag{22}$$

The term *safety* comes from Magnetohydrodynamics, MHD, where the safety factor is related to plasma stability [5].

V. Numeric Implementation

A. The MATLAB® Environment

The simulation environment, developed to compute the magnetic field inside the Tokamak and to solve the particle

TABLE I
EXPERIMENT PARAMETERS BASED ON THE TEXTOR TOKAMAK.

Name	Denotation	Value
Major radius	R_{ma}	1.75 m
Minor radius	R_{mi}	0.47 m
Toroidal field coils	N	16
Winding per coil	N_W	≈ 60
Toroidal coil current	I_C	≈ 27 kA
Plasma current	I_P	800 kA

orbit, is described in full detail in appendix A. The environment mainly consists of the following components:

- One script for invoking the different routines in correct order and for basic user input.
- Two input functions for loading of physical constants, e.g. the permeability of vacuum, and machine parameters. The input functions can be edited in order to change simulation parameters, e.g. simulation time and driven plasma current.
- Four functions for computing the magnetic field at a spatial point in the Tokamak.
- One function for computing the initial velocity of the particle.
- One function for invoking the numeric differential equation solver. Can be edited in order to set the solver's numerical parameters, e.g. relative tolerance and maximum step length.
- One function for computing of the particle guiding centre path, given the true particle path returned by the solver.
- One function for generating three dimensional plots and two dimensional projections of the particle orbits.

As a compliment to the developed environment, a series of analysing scripts were developed to collect and compare data from different simulations.

B. Construction Parameters

In order for the model to generate realistic results, the experimental parameters are based on the physical construction of the TEXTOR Tokamak, located at Forschungszentrum Jülich in Germany [7]. Experiment parameters used in the model are presented in table I.

The toroidal coil current, I_C, is calculated using the fact that the toroidal magnetic field on the magnetic axis within the TEXTOR Tokamak is 3 T [7]. The number of windings per toroidal field coil is an approximate number due to the fact that the data was obtained orally from an engineer at the TEXTOR facility during a visit to Forschungszentrum Jülich, Germany.

C. Particle Parameters

For the sake of simplicity and easier analysis of the simulation results, the initial position and the thermal energy of the plasma particle are fixed during all simulations analysed in this report. The particle simulated is a proton throughout all simulations. All initial condition and particle parameters are presented in table II.

TABLE II
INITIAL CONDITION AND PARTICLE PARAMETERS

Name	Denotation	Value
Energy	E	20 keV
Mass	m_p	$\approx 1.6726 \cdot 10^{-27}$ kg
Charge	e	$\approx 1.6022 \cdot 10^{-19}$ C
Toroidal angle	ϕ	0 rad
Poloidal angle	θ	0 rad
Poloidal radius	r	$R_{\text{mi}}/2$ m
	$x(\phi, \theta, r)$	$R_{\text{ma}} + R_{\text{mi}}/2$ m
	$y(\phi, \theta, r)$	0 m
	$z(\phi, \theta, r)$	0 m
Pitch angle	φ_p	$0.1\pi \leq \varphi_p \leq 0.5\pi$ rad

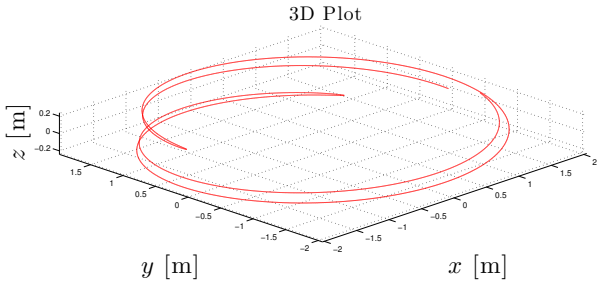

Fig. 9. Three dimensional plot of particle path with TEXTOR based simulation parameters and $\varphi_p = 0.1\pi$.

VI. RESULTS & ANALYSIS

A. TEXTOR based simulation

If all parameters are fixed according to table I and II and the pitch angle is selected to be $\varphi_p = 0.1\pi$ the resulting particle orbit is presented in figure 9.

The path in figure 9 shows that the particle performs bounces when the poloidal angle, θ, reaches a certain point, $\theta = \pm\theta_b$. This is better visualized if the particle path is projected to a two dimensional plot. The projection is achieved by performing the mapping described in (23).

$$\begin{cases} R(x, y, z) = \sqrt{x^2 + y^2} \\ z(x, y, z) = z \end{cases} \tag{23}$$

The two dimensional projection with the TEXTOR based parameters and $\varphi_p = 0.1\pi$ is presented in figure 10. If the two dimensional projection of the particle path displays the trapped behaviour illustrated in figure 10 the particle is referred to as *trapped* since its guiding centre doesn't perform circular orbits around the centre of the torus cross section.

The trapped behaviour depicted in figure 10 is caused by the inhomogeneous magnetic field. The magnetic field gradient points towards the z-axis and therefore the magnetic pressure, described in (24), increases as the particle moves towards smaller R.

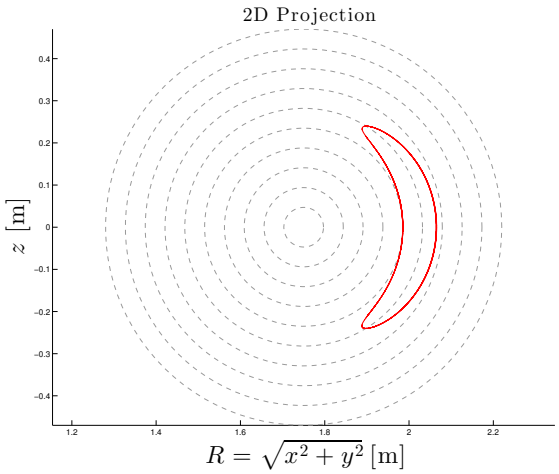

Fig. 10. Two dimensional projection of particle path with TEXTOR based simulation parameters and $\varphi_p = 0.1\pi$. The dashed lines are a representation of the different magnetic flux surfaces.

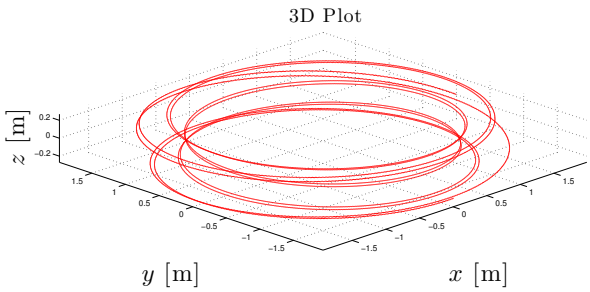

Fig. 12. Three dimensional plot of particle path with TEXTOR based simulation parameters and $\varphi_p = 0.3\pi$.

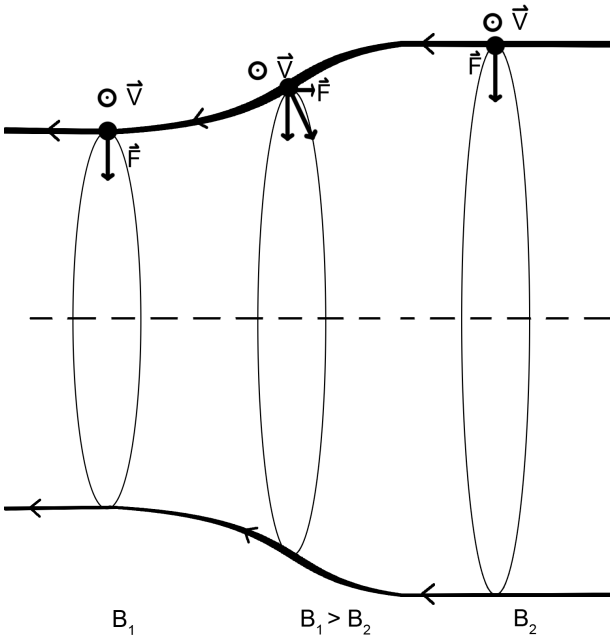

Fig. 11. The resulting force on particles gyrating in a magnetic field of constant and changing magnetic field density.

$$P_m = \frac{|\vec{B}|^2}{2\mu_0} \tag{24}$$

The increasing magnetic pressure is related to the increasing density of the magnetic field, $|\vec{B}|$. This increasing density is illustrated by a compression of the magnetic field lines. This effect causes the particle not only to accelerate towards the guiding centre, but also in the direction reverse that of the magnetic field gradient. A graphic representation of this effect is displayed in figure 11.

If the particle follow the field lines in a magnetic field with an increasing magnetic field strength, its parallel velocity will decrease due to the force experienced by the particle. If the initial parallel velocity is small, the parallel velocity will decrease and finally reverse its direction due to the acceleration. If the particle has a large parallel velocity, it will be able to overcome the increasing magnetic pressure and continue its parallel motion after the magnetic compression occurred. However, its parallel velocity is smaller after traversing this magnetic threshold.

During the motion inside the Tokamak, the particle will be affected by the magnetic drift and will move from one flux surface to another. When the particle changes flux surface, the magnetic field affecting it changes and makes the particle following a new field line. It is this difference in flux surface, that creates the characteristic shape depicted in figure 10.

If the pitch angle is increased, e.g. to $\varphi_p = 0.3\pi$, the ratio between the parallel and perpendicular velocity of the particle increase and this makes the particle able to move along the field line and overcome the magnetic pressure. The resulting projected particle path is an approximate circle. An example of such a *passing* particle orbit is depicted in a three dimensional plot and a two dimensional projection in figure 12 and 13, respectively.

1) The Confinement Width: In order to relate the different particle orbits to the concept of confinement, it is essential to define a numerical measurement of how well the particle is confined. A simple, yet intuitive measure, is the maximal confinement width defined by equation (25).

$$w = \max(r) - \min(r) \tag{25}$$

The confinement width can be seen as the particles tendency to move across different flux surfaces during a transit- or bounce period, i.e. during the time to complete one circular revolution around the magnetic axis (transit period) or one complete bouncing orbit at the side of the magnetic axis (bounce time). If the confinement width is large, the particle traverses a large set of flux surfaces and if $w \to 0$ the particle is fixed to move along one flux surface. The confinement width is displayed for a trapped and passing particle orbit in figures 14 and 15 respectively.

In the field of fusion, the level of confinement is the ability to retain particles within the plasma and prevent them

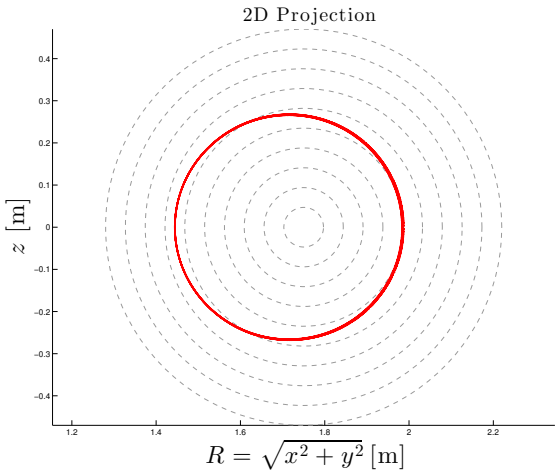

Fig. 13. Two dimensional projection of particle path with TEXTOR based simulation parameters and $\varphi_p = 0.3\pi$. The dashed lines are a representation of the different magnetic flux surfaces.

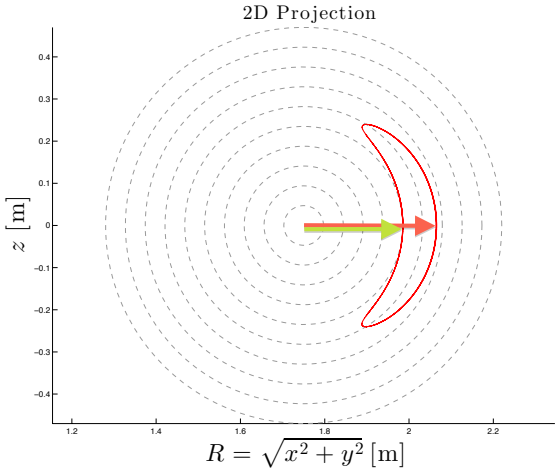

Fig. 14. Representation of max(r) (long arrow) and min(r) (short arrow) for a trapped particle orbit.

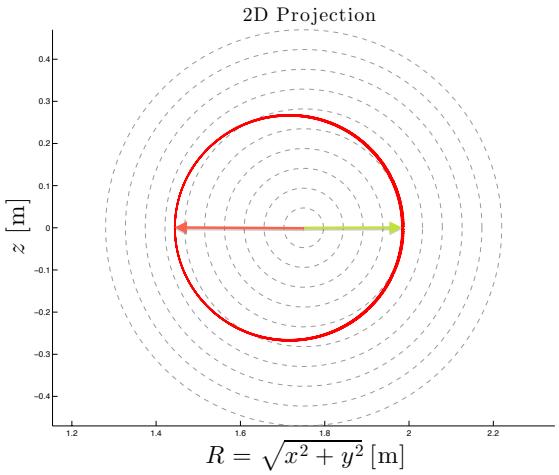

Fig. 15. Representation of max(r) (long arrow) and min(r) (short arrow) for a passing particle orbit.

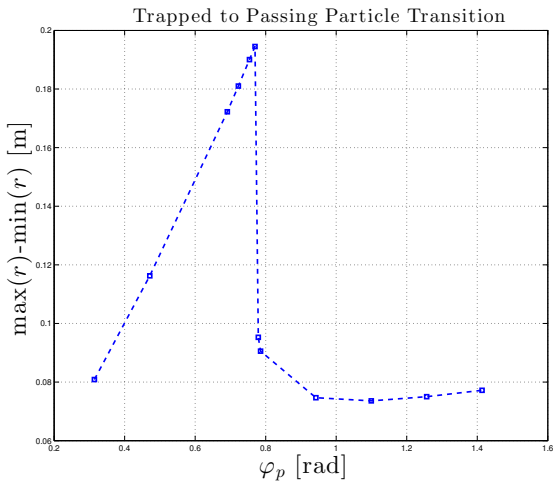

Fig. 16. Confinement width, w, as a function of pitch angle, φ_p, with TEXTOR based simulation parameters.

from touching the plasma vessel. Particles leaving the plasma and interacting with the wall makes the plasma lose thermal energy.

If a particle is confined within the magnetic field, it will not lose confinement according to the model developed in this report, since collisions and other transport effects are not taken into account. However, if a plasma particle is subjected to a collision, its orbit may shift towards the vessel wall. If the particle is repeatedly subjected to collisions, its orbit will move closer to the wall and finally, intersect the vessel wall, leading to the loss of the plasma particle. The distance of the orbital shift a particle is subjected to is proportional to its orbital width, i.e., its confinement width, w.

A large confinement width makes the particle lose confinement after a relatively small number of collisions, whilst particles that experience a small confinement width requires a larger amount of collisions in order to lose confinement. A small confinement width is therefore desired.

B. Pitch Angle Relationship

The different particle behaviours in figures 10 and 13 suggests that the particle motion is dependent on the pitch angle, φ_p, i.e. the initial condition of the particle. At a low pitch angle the particle becomes trapped and at a large pitch angle, the particle becomes passing. In order to find the angle of behaviour transition, φ_T, the confinement width is studied as function of the pitch angle. The result is shown in figure 16.

Figure 16 shows that a trapped to passing behaviour threshold is present somewhere in the the interval $\varphi_p \approx 0.24\pi \approx 0.75$ when TEXTOR based simulation parameters are used. More importantly, at the point of behaviour transition, the confinement width is approximately halved meaning that the confinement width of the trapped particle just before the point of transition is double that of the passing particle confinement width just after point of transition. This transition behaviour is easier to interpret if a two dimensional projection of a particle

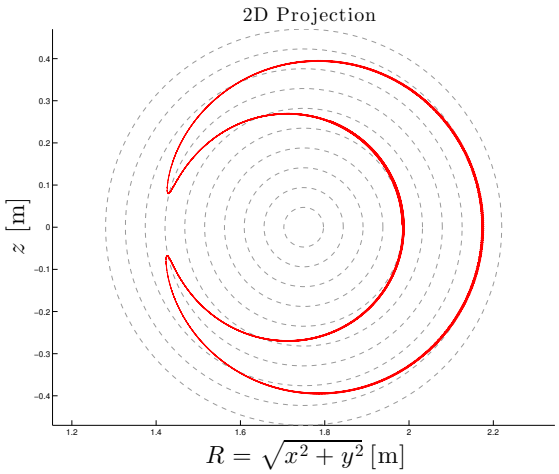

Fig. 17. Two dimensional projection of particle orbit using $\varphi_p = 0.245\pi$ and TEXTOR based simulation parameters.

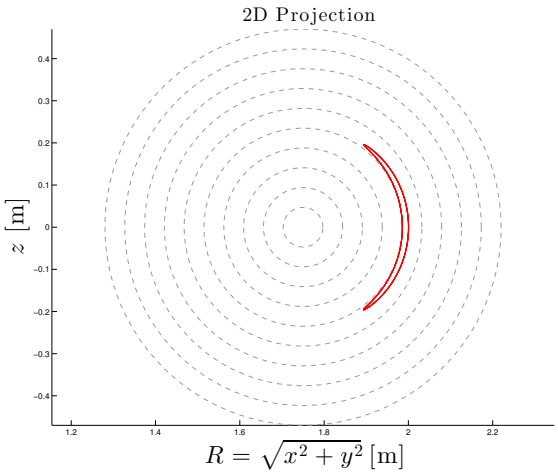

Fig. 19. Two dimensional projection of particle orbit with $\varphi_p = 0.1\pi$, $I_P = 4\,\mathrm{MA}$ and otherwise TEXTOR based parameters.

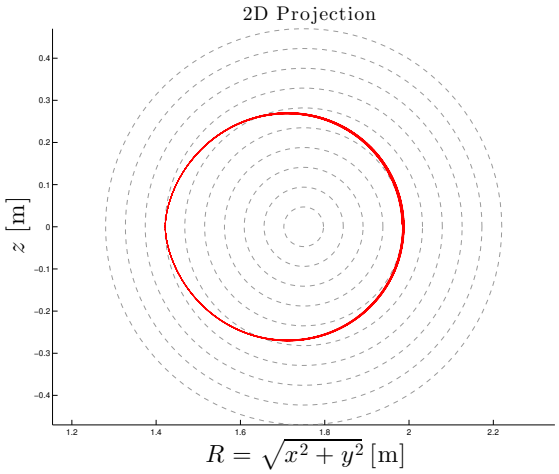

Fig. 18. Two dimensional projection of particle orbit using $\varphi_p = 0.248\pi$ and TEXTOR based simulation parameters.

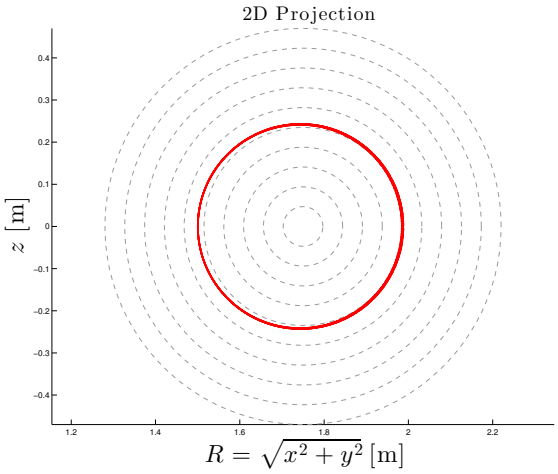

Fig. 20. Two dimensional projection of particle orbit with $\varphi_p = 0.3\pi$, $I_P = 4\,\mathrm{MA}$ and otherwise TEXTOR based parameters.

orbit with pitch angle close to the angle of transition is studied. A two dimensional projection using $\varphi_p = 0.245\pi$ is shown in figure 17.

Figure 17 shows, that the particle almost performs a circular loop before it bounces and traverses a different flux surface in the backwards direction. If a pitch angle is selected so that it's slightly larger, the inner circular loop will be fully completed, leading to the passing particle behaviour depicted in figure 18. The ratio between the confinement width in figure 17 and 18 is approximately two.

C. Plasma Current Relationship

Since the plasma current generates the poloidal magnetic field inside a Tokamak, it may be an important factor concerning plasma confinement. In order to examine the relationship between the plasma current and single particle confinement, the confinement width is studied as a function of an increasing plasma current. A set of two dimensional particle projections for a trapped and passing particle with a fivefold larger plasma current is depicted in figure 19 and 20 respectively.

Figure 19 and 20 shows that the trapped particle orbit projection becomes more compressed, and the particle traverses a smaller number of flux surfaces. For the passing particle, the projected orbit asymptotically becomes a circle with its centre at the magnetic axis. The behaviour shows that the confinement width decreases as the plasma current increases. The dependency is depicted in figure 21 and 22.

Figure 21 and 22 shows that the confinement width decrease as the plasma current increases. In order to set up a model to describe this relationship, the *transit time* for a particle is studied.

The transit time is the time it takes for a particle to complete one bouncing or passing orbit and can be estimated as

$$T_{\text{transit}} \approx \frac{L}{v} = \frac{2\pi Q R}{v} \tag{26}$$

where L is the orbit length and v is the guiding centre velocity during the transit motion and can be approximated as the mean of the parallel velocity, $v \propto \langle v_{\|} \rangle$. The confinement width is now considered as a function of the magnetic drift velocity,

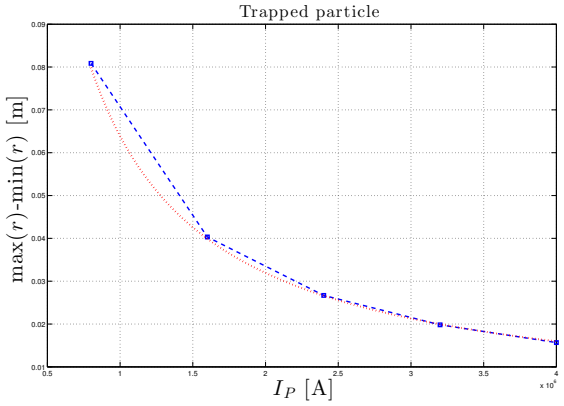

Fig. 21. Relationship between the confinement width, w, and the plasma current, I_P, when $\varphi = 0.1\pi$ and otherwise TEXTOR based parameters are used. Dotted line represents fitted analytic inverse function.

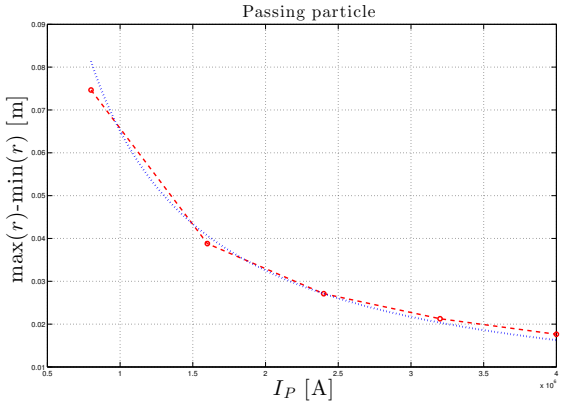

Fig. 22. Relationship between the confinement width, w, and the plasma current, I_P, when $\varphi = 0.3\pi$ and otherwise TEXTOR based parameters are used. Dotted lined represents fitted analytic inverse function.

$\vec{v}_D$.

$$w \propto v_D T_{\text{transit}} = v_D \frac{L}{v} \tag{27}$$

Using equation (21), i.e. $v_D \propto v^2 (RB)^{-1}$, and the earlier mentioned orbit length, the confinement width can be expressed as

$$w \propto \frac{v^2}{BR} \frac{QR}{v} \propto \frac{Q}{B} \tag{28}$$

or

$$w \propto \frac{rB}{RB_\theta} \frac{1}{B} \propto \frac{1}{B_\theta}. \tag{29}$$

Finally, since the poloidal magnetic field is proportional to the plasma current $w \propto I_P^{-1}$. From this relationship, a simple one parameter model described in (30) can be used to estimate how well the simulation data fits the model.

$$w = \frac{k}{I_P} \quad \Leftrightarrow \quad k = I_P w \tag{30}$$

All data points provided in figure 21 and 22 are used to generate a series of estimates of parameter k. The two series of k-estimations, one for the trapped particle and one for the passing particle, are then analysed using relative standard

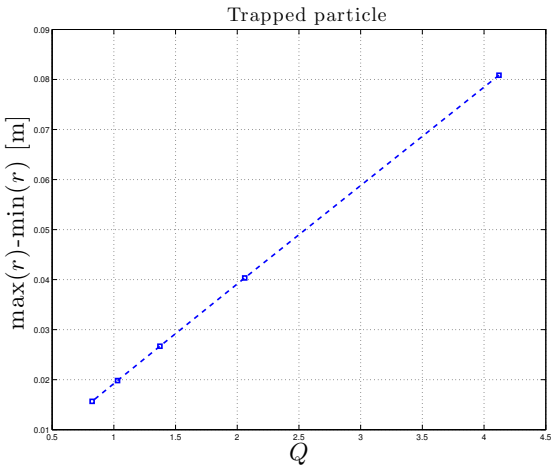

Fig. 23. Dependency between the confinement width, w, and the safety factor, Q, when $\varphi_p = 0.1$ and otherwise TEXTOR based simulation parameters are used.

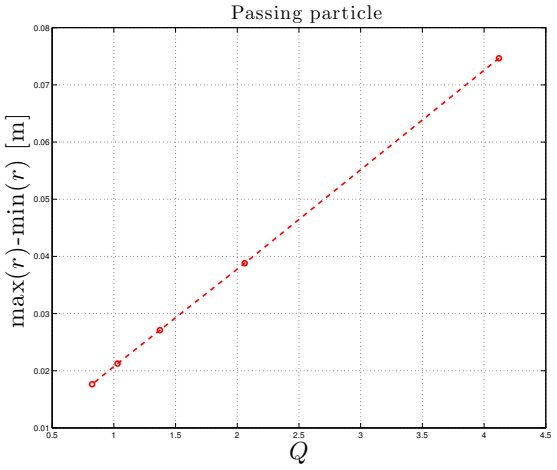

Fig. 24. Dependency between the confinement width, w, and the safety factor, Q, when $\varphi_p = 0.3$ and otherwise TEXTOR based simulation parameters are used.

deviation. The resulting deviations are 1.3 % for the trapped particle dependency and 6.7 % for the passing particle. This data leads to the conclusion, that the dependency between the confinement width and the plasma current are inversely proportional.

If the relationship between the safety factor, which is recursively dependent on the plasma current, and the confinement width is studied, the result is a linear dependency as depicted in figure 23 and 24.

Since the safety factor is defined according to equation (28), the linear dependency between the safety factor and the confinement width confirms that the relationship between the confinement width and the plasma current is indeed an inverse relationship.

VII. Conclusions

In this report, an analytic model for computing the orbit of a single charged particle within a toroidal fusion device

with properties similar to that of a Tokamak has been developed. The model has been numerically implemented using MATLAB® software and utilized to perform a series of numerical studies concerning the particle orbit response to changes in input parameters, i.e. changes in machine configuration and particle initial conditions.

The studies have shown that the particle displays different motion behaviours due to differences in the initial conditions and is therefore dependent on the particle motion relative to the surrounding magnetic field. The studies also showed that the type of particle behaviour, i.e. *trapped* or *passing*, is independent of the driven plasma current.

At the point of transition between the *trapped* and *passing* particle behaviour, the confinement width is approximately halved.

A larger plasma current improves the particle confinement within a Tokamak, and the relationship between the confinement width and the plasma current is sufficiently modelled using the inverse function, i.e. $w \propto I_P^{-1}$.

ACKNOWLEDGEMENTS

First and foremost, I would like to thank my supervisors Thomas Johnson and Simon Tholerus at the department of Fusion Plasma Physics, for always providing me with excellent feedback in generous amounts and introducing me to the field of fusion and the science of plasma physics.

I would also like to thank Marek Rubel and Darya Ivanova at the department of Fusion Plasma Physics, for broadening my perspective in how the field of fusion is being researched during a visit to Forschungszenrum Jülich in Germany.

REFERENCES

[1] L. Clarke, J. Edmonds, V. Krey, R. Richels, S. Rose, and M. Tavoni, "International climate policy architectures: Overview of the emf 22 international scenarios," *Energy Economics*, vol. 31, Supplement 2, no. 0, pp. S64 – S81, 2009, international, U.S. and E.U. Climate Change Control Scenarios: Results from EMF 22. [Online]. Available: http://www.sciencedirect.com/science/article/pii/S0140988309001960

[2] (2013, january) Iter organization. [Online]. Available: http://www.iter.org/proj/iterandbeyond

[3] Y. Shimomura, "Preparation of iter construction and operation," *Fusion Engineering and Design*, vol. 81, no. 1-7, pp. 3 – 11, 2006/02/. [Online]. Available: http://dx.doi.org/10.1016/j.fusengdes.2005.06.358

[4] (2013, march) European fusion development agreement, efda. [Online]. Available: http://www.efda.org/fusion/focus-on/limiters-and-divertors/

[5] J. P. Freidberg, *Plasma Physics and Fusion Energy*. Cambridge: Cambridge University Press, 2007.

[6] (2013, april) Wikimedia commons. [Online]. Available: http://en.wikipedia.org/wiki/File:Lorentz_force.svg

[7] (2013, april) Jülich forschungszentrum, institut für energie- und klimatforschung, plasmaphysik (iek-4). [Online]. Available: http://www.fz-juelich.de/iek/iek-4/DE/Forschung/09_TEXTOR/_node.html

[8] (2013, april) Wikimedia commons. [Online]. Available: http://upload.wikimedia.org/wikipedia/commons/1/17/Torus.png

[9] (2013, april) Wikimedia commons. [Online]. Available: http://en.wikipedia.org/wiki/File:Electromagnetism.svg

[10] P. C. Matthews, *Vector Calculus*. London: Springer, 2005.

[11] (2013, april) Mathworks documentation center. [Online]. Available: http://www.mathworks.se/help/matlab/ref/atan2.html

[12] (2013, april) Wikimedia commons. [Online]. Available: http://en.wikipedia.org/wiki/File:Electromagnetism.svg

[13] (2013, april) Wikimedia commons. [Online]. Available: http://en.wikipedia.org/wiki/File:Charged-particle-drifts.svg

[14] F. F. Chen, *Introduction to Plasma Physics and Controlled Fusion*. New York: Plenum Press, 1984.